MICROBUBBLE GENERATION BY FLUIDICS.
PART I: DEVELOPMENT OF THE OSCILLATOR

Václav Tesař
Institute of Thermomechanics v.v.i., Academy of Sciences of the Czech Republic, Prague

Abstract: In current research project the author investigates generation of sub-millimetre air bubbles in water. This is not an easy task: usual bubble size is several millimetres and known methods of making them smaller, which would bring advantages in many technological processes, are not economical. A non-expensive way to generation of microbubbles was found in pulsating the supplied air flow, using a no-moving-part fluidic oscillator. The project involves two separate problems: (a) Developing a suitable fluidic oscillator for frequency $200 - 300$ Hz, with minimised hydraulic losses. (b) Understanding the pulsatile bubble formation mechanism and using the knowledge in aerator design. This paper discusses the author's solution of the first problem, development of the oscillator – which resulted in a device with behaviour different from what has been so far described in literature.

1. Introduction

To those who do not follow recent developments in industrial processes involving gas bubbles in liquids may come as a surprise the wide variety of applications and rapidity of the progress in this field. Bubbles are the key factors in wastewater treatment [30], paper manufacture and recycling with ink removal [32], oxidative leaching of plutonium [2], photoresist removal from silicon wafers [31], separation or concentration of various materials by froth flotation [8], yeast production [4], hydrodynamic power recovery, growing unicellular organisms [5], sonochemical synthesis [3], production of biopharmaceuticals [8], salvaging remaining crude oil from „exhausted" oil wells, and extracting liquid fuels from bituminous tar sands (— which is immensely important since tar sands are estimated to contain more than two-thirds of total global fossil fuel deposits exploitable in near future [9]). Because of the obvious advantages associated with small bubbles' high surface-to-volume ratio (which is an essential factor in diffusive transport) and slow velocity of rising to the surface (giving more time for the transport), interest concentrates on sub-millimetre microbubbles. Recent literature discusses even sub-micron size nanobubbles [1], which can stay suspended in the liquid, agitated by Brownian motion, for time scale as long as of the order of days — but some of their aspects are rather enigmatic and controversial and therefore out of question in this project. Of course, bubbles tend to grow by mutual agglomeration. The smaller is the initial size, the longer remain bubble diameter small and this is another reason for concentrating on the generation of bubbles that were as small as possible.

The most straightforward method how to get air (or other gas) in the form of bubbles into a body of liquid is blowing it, under pressure, through orifices in a component called aerator – usually just a system of parallel small orifices located at the end of the supply tube. The desirable sub-millimetre bubble size is, however, more than an order of magnitude smaller than what is obtainable with a commonly used standard aerator, even if its exit orifices were of sub-millimetre size. To meet the micro-bubble requirements, it is necessary to introduce new generation methods.

One can still encounter the naive approach that small bubbles would result if the used aerator simply has very small exit orifices. Unfortunately, due to the basic aspects of the Young-Laplace law, which governs the surface tension that plays the decisive role in the bubble formation, the bubbles growing at the aerator exits are subject to instability: all the bubble growth concentrates to a few exit orifices, in which the bubbles can reach size substantially larger than the orifice diameter. There is actually a number of known methods generating real microbubbles - but unfortunately only a few of them are economically viable. As an example, very small bubbles can be produced by action of ultrasound, but it is too expensive for use in large-scale industrial processes. An attractive solution was currently found in pulsating the bubbles in the process of their generation at the aerator exit. Considering factors like cost, reliability, life, and robustness, the best way of generating the oscillation is use of no-moving-part fluidic oscillators [10, 6]. They are noting more than just fixed-geometry cavities using hydrodynamic instability in the flowing gas – usually augmented by providing suitable feedbacks. As a matter of fact, the basic ideas upon which these oscillators are based are by no means new. They have been known for at least 50 years. Nevertheless, they became nearly forgotten. The reason was mainly the

role for which these devices were initially developed: an application in fluidic logic circuits [11]. This has led to a dead end because information processing is more effectively handled by electronics, with which the information-processing fluidics was unable to compete.

A typical effect of applied oscillation is documented in ref. [12]. The aerator discussed there had really very small equivalent diameter size of exit orifices: $38\mu m$. However, with steady air flow the bubbles produced were of average size $1\,059\mu m$ (not fitting into the microbubble definition). They were actually 28-times larger than the orifice. With the fluidic oscillator, the bubble size with the same aerator decreased to $86\mu m$, which is only approximately twice the orifice size.

Author of the present article has recently received a TAČR research grant for a project aimed at generation of microbubbles, to be applied to biogas upgrading (removal of CO_2 and increasing CH_4 concentration to a level high enough for the biogas suitable to substitute natural gas in standard gas net). The generation of microbubbles, on the lines similar to those discussed in [5], is requested and is to be based on the use of fluidic oscillators.

The project thus involves two tasks, both quite difficult:
(a)   Developing a suitable fluidic oscillator.
(b)   Obtaining an understanding of the bubble formation mechanism under the influence of applied oscillation and designing an aerator on the basis of this acquired knowledge.

The present paper discusses the first of these problems: the development of the model oscillator used in the laboratory tests.

2   Fluidic oscillators

At the present initial stage of the project, the parameters of the generated oscillation – frequency and amplitude - are not yet defined. It is expected that the optimum values will be found in the experiments with bubble generation. There are, however, several requirements which are obvious. It is, of course, the capability to generate the oscillation without an action of moving or deformed component parts inside the device (which would inherently limit the oscillator life, reliability, and maintenance-free operation under water). The oscillator is expected to be immersed in water since it has to be immediately side-by-side with the aerator – otherwise the oscillation would be severely damped in the interconnecting tubing (the aerator is to be placed at the bottom of the liquid tank so that the diffusion of the gas into liquid takes place during the bubble rising to the surface). The absence of inertia of moving parts should ensure an operation of the oscillator at high frequency without wear or material fatigue of components. Some previous experience was, in fact, already obtained by the author as described in [5], [6], and [7], and it suggests the suitable frequency is likely to be at about $200 - 300\,Hz$. This is the frequency range in which a mechanical moving component would soon deteriorate. Because of the uncertainty concerning the proper frequency value, priority was to be given to the oscillator principles that allow for simple frequency adjustment. Such adjustment is rather simple in those oscillator principles that work with external, easily accessible and adjustable feedback loops.

Another essential requirement is economy of operation. In fact, compared with e.g. ultrasound bubble generation, efficiency of using fluidics may become one of decisive factors. The compressed air is expensive, however, so that the magnitude of hydraulic losses inevitably associated with the air flow through the device is to be as low as possible. It will be an advantage if the oscillator geometry can avoid complex internal flow passages with sharp turns, sharp edges causing separation of flow from the channel walls, and high flow velocities. If the working principle would necessitate accelerating the air flow to high velocity, the design must make possible inclusion of diffusers or similar components ensuring pressure recovery [25] taking place immediately downstream.

2.1. Survey of oscillator principles

A list of principles on the basis of which it is possible to design a no-moving-part fluidic oscillator is presented in Fig. 1. No such survey of principles has been found in available literature and this list thus may be the first attempt at classification of the fluidic oscillator ideas. As such, it may have the disadvantages typical of first attempts: it may be not fully exhaustive and, on the other hand, perhaps some of the principles in the list may be not mutually exclusive.

The first principle on the list in Fig. 1 is the use of extraordinary characteristic of some (very rare) fluidic devices. The characteristic is the dependence between the pressure drop on the device and the flow rate passing through it. In the top part of Fig. 2, an example of such a characteristic is plotted in relative co-ordinates. The capability of generating periodic unsteadiness is associated with negative slope of the characteristic: pressure drop decreasing in the flow rate grows. From the energy conservation point
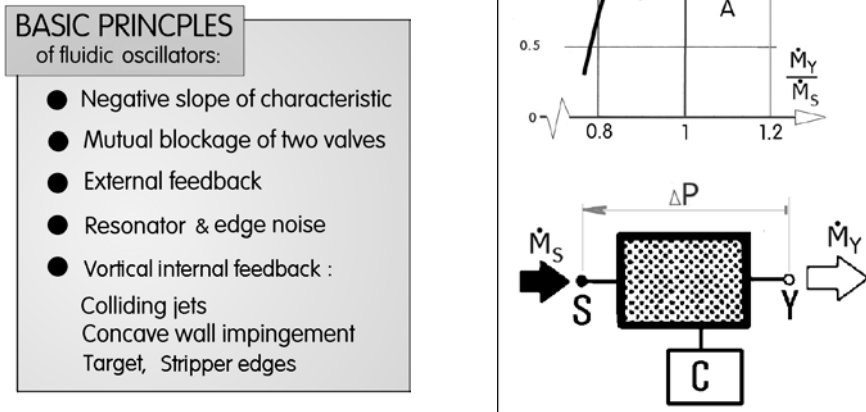
Fig. 1 (Left) List of operating principles on which are based most known fluidic oscillators. The choice of items in this list is somewhat arbitrary – in most of them it is usually possible to identify some form of feedback loop.

Fig. 2 (Right) If there is an interval with negative slope on a device characteristic, as in the example on top, it is usually possible bring the device into sustained oscillation – perhaps with the assistance of temporary fluid storage during a part of the cycle in the accumulation chamber C.

of view it is apparent that the negative slope may exist, if at all, only on a rather small segment of flow rates and certainly not along the whole extent of the characteristic. If such a segment is found, then the principle of oscillation generation has the undeniable advantage of utmost simplicity. It needs not to be said that such behaviour is extremely rare. It may be set up with moving components, utilising for example the "*Aerodynamic paradoxon*" phenomenon [26, 27]. In the realm of pure, no-moving-part fluidics the only useful case seems to be the circuit according to the patent [13], which employs a spectacular property of some vortex amplifiers (which, being three-terminal devices, are much more complex than the two-terminal device schematically presented in Fig.2.

The essential fact is the negative slope of characteristic is unstable. Let us assume the state O on the characteristic in Fig. 2. If the mass flow rate $\dot{M}$ of the fluid slightly increases due to some external disturbance, the pressure drop ΔP becomes slightly lower than ΔP_0. This makes the flow easier – so that the flow rate $\dot{M}$ increases even more, making the fluid flow even easier, until the process stops in the state A. On the other hand, any accidental decrease of the flow rate increases the pressure drop, the process spiralling to the state B. The regimes between A and B are inaccessible.

Let us now assume a situation where the fluid flow previously accumulated in the accumulation chamber C leaves the chamber and is added to the output flow rate $\dot{M}_Y$ - so that this flow is larger than the supply flow $\dot{M}_S$ to the degree of the instantaneous state being represented by an operating point on the characteristic laying on the positively sloping branch at right from the point A. The amount of fluid available in C is, of course limited. As the emptying of the chamber C progresses, the operating point moves down the positively sloping branch until it and reaches the point A. Any further progress along the negatively sloping part of the characteristic is impossible, because the instability explained above. What happens is the state of the device switching along the dashed horizontal line to the positively sloping branch of the characteristic at left from the point B. There, however, the characteristic shows the output flow rate $\dot{M}_Y$ to be smaller than the supply flow $\dot{M}_S$. The difference between them is stored in the chamber C. The storage capability being limited, the flow into C gradually decreases and the operating state now climbs up to the point B. From there it switches along the upper dashed horizontal line to the right-hand side, where the process repeats itself by gradual discharge from C.

Similarly very rare are examples of fluidic oscillators employing a pair of flow control valves blocking one another's output flow, Fig. 3, in analogy to the unstable version of the Eccless-Jordan multivibrator. The use of the pair of vortex amplifiers in [28] seems to be the only reference in literature about the otherwise quite obvious fluidic analogy, Fig. 4. Apparently it seems to be un-economical to use
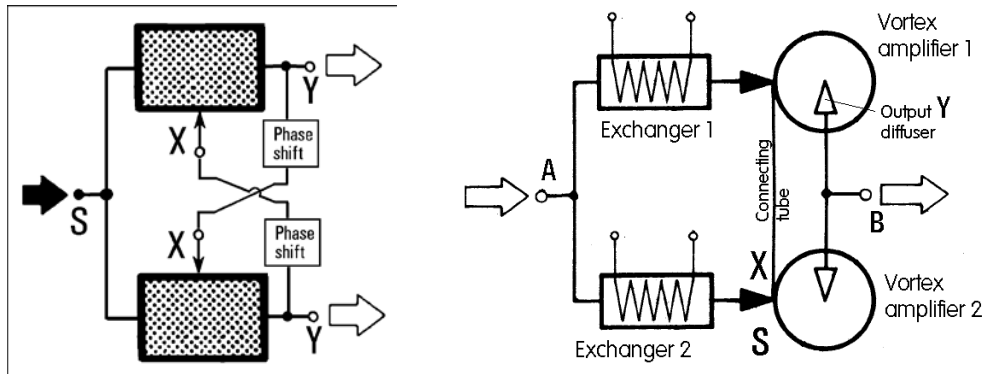
Fig. 3 (Left) The oscillator principle with alternating mutual blockage of flow control valves. This is a direct analogy to the Eccless-Jordan circuit from early history of electronics [14]. In the stable regime it used to serve as a binary memory element. In the unstable configuration it is called multivibrator because of the wide frequency spectrum of the output signal.

Fig. 4 (Right) Present author has used the mutual blockage multivibrator [28], with vortex amplifier valves, for enhancing the heat transfer in heat exchangers.

two amplifying valves in an application know to be manageable with only a single flow amplifying valve. In Fig. 4, the two heat exchangers and two cylindrical vortex chamber form the two parallel arms of a Wheatstone bridge supplied by the pressure difference between A and B. A simple connecting tube represents the diagonal of the bridge. Both ends of the tube, upper and bottom one, enter as tangential control inlets into the respective vortex chambers in tangential direction. As is generally known, the vortex valve exhibits a high value of the pressure drop across the vortex chamber, between the radial supply nozzle S and the diffuser in the output Y , in the presence of tangential flow into the inlet X. Let us, e.g., assume this turned-down state exists in the vortex amplifier 2 in Fig. 4 while the flow through the other vortex amplifier 1 is easy. This means there is a large flow through the exchanger 1, with consequent large pressure drop on it, and small flow through exchanger 2. At the exit of the exchanger 1 the pressure is nearer to the lower level in B while at the exit from exchanger 2 the pressure is nearer to the higher level A. This pressure difference generates a flow through the connecting tube (diagonal of the bridge). This flow enters tangentially into the vortex amplifier 1. After a certain time lag (needed for the flow spin-up in amplifier 1), the vortex amplifier 1 is turned down and vortex amplifier becomes open. Now in the exit of the closed exchanger 1 the pressure is nearer to the high pressure level in A while at the exit from exchanger 2 the pressure is nearer to the low pressure in B. The direction of the pressure difference across the connecting tube is reversed – and also reversed is the flow in it, towards the amplifier 2. This becomes closed and the whole circle of events is repeated.

While the principles discussed so far were of more or less academic interest, the next step in Fig.1, amplifiers with feedback loop, are the mainstay of present-day fluidics. A part of the output flow in Y is taken back by this loop into the control terminal, Fig. 5. Because of the amplifying properties of the fluidic valve (presented schematically as a " black box" in this diagram) even a weak signal at X suffices for decreasing the output flow: this feedback is described as a negative one. It may be imagined that the fluid supplied into S is left to leave through the vent V. As a result, nothing gets into the feedback loop, the action of which ceases for some time determined by the phase-shift element. The flow into Y can increase – and the repetition of the process begins.

How this oscillatory phenomenon takes place may be easier to show in the case of the Coanda-effect valve presented schematically in Fig.5. This is a jet-deflection type valve. The main fluid flow supplied into S leaves the supply nozzle (symbol: black triangle) as a jet which due to the Coanda-effect attaches always to the preferential attachment wall. It is captured by the collector (white triangle – it contains a diffuser that converts the kinetic energy of the jet back into the pressure) and leaves through the output terminal Y. As in previous Fig. 5, a part of the output flow from Y returns by the feedback loop and enters the control terminal X. Amplifying properties of the jet-deflection valves are based on the fact that a small flow from the control nozzle X (the other black triangle) can cause detachment of the flow from the preferential attachment wall. The main flow can adhere to the auxiliary attachment wall (it is smaller or placed further away from the main flow path) that directs it into the vent V. No phase shift device is shown in Fig. 6 because the inertance of the fluid in the feedback loop channel itself sufficed for generating the delay.
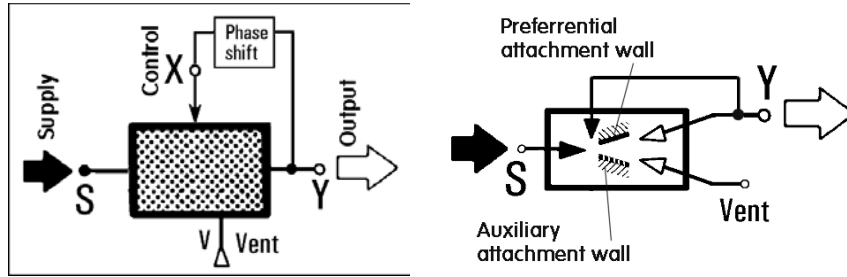
Fig. 5 (Right)   Conceptually most obvious classical principle of an oscillator using the amplification properties of a fluidic valve.

Fig. 6 (Left)   Schematic representation of a feedback-type oscillator from Fig. 4 with monostable jet-deflection amplifier using the Coanda-effect attachment to attachment walls.
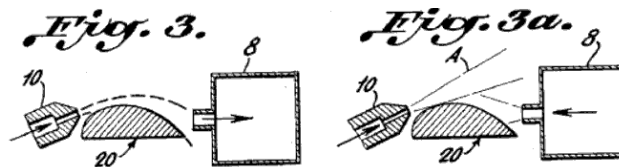

Fig. 7   Relaxation-type oscillator with jet attachment filling an accumulation chamber and separation of the jet by the control action of the flow from the emptied chamber – original pictures from Zalmanzon's Patent [15].
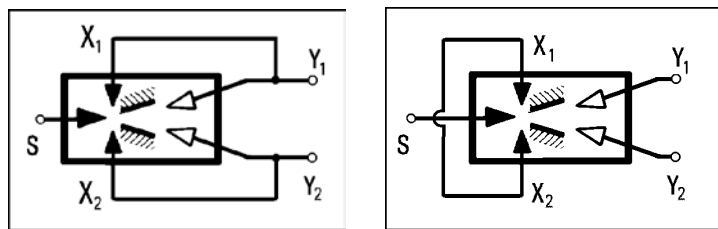

Fig. 8 (Left)   The most popular among the fluidic oscillator configurations with external feedback is the Warren's [17] layout with symmetric bistable amplifier and two feedback loops.

Fig. 9 (Right) Somewhat more sophisticated feedback layout with a single loop connecting the control terminals X_1 and X_2. The flow in the loop is generated by the pressure difference across the deflected jet – the difference which holds it at its attachment wall. Often described in literature as Spyropoulos-type feedback, it was in fact also invented by Warren, already in 1960 [16].

As a matter of fact, some feedback loop may be almost always detected in all the other fluidic oscillators – where, however, it usually does not have the form of a channel leading to the control nozzle . It may be simply a cavity in which a part of the flow can turn back in a stationary vortex or eddy. Sometimes the accumulation chamber as the chamber C in Fig. 4 periodically filled and emptied is present or may be identified in some part of the amplifier cavity. An example of classical oscillator which it may be difficult to put into any of the lines of Fig. 1 is presented in Fig. 7. There is immediately apparent the main nozzle (10) and the preferential attachment wall (20 - the other, auxiliary attachment wall is missing completely) and the accumulation chamber (8). In fact, this is a case belonging to the jet-deflection oscillators similar to the one from Fig. 6, but the feedback loop here degenerated and the control nozzle temporarily changes role with the preferential collector.

The two most often used oscillator layouts are presented schematically in Figs. 8 and 9. The basic component in both cases is a symmetric bistable jet-deflection amplifier with equal opportunity of the main jet to attaching to any of the two opposite attachment walls. Again, the mutual relations between various principles listed in Fig. 1 shows the contamination of ideas. The configuration in Fig. 8 may be seen as essentially the Jordan-Eccless connection of two valves from Fig. 6.

A different oscillation mechanism, at the fourth line of the list in Fig. 1, although also based on switching the main jet in a Coanda-effect jet-deflection valve is shown in Fig. 11. It is closely related to some musical instruments such as the one shown in Fig. 10.
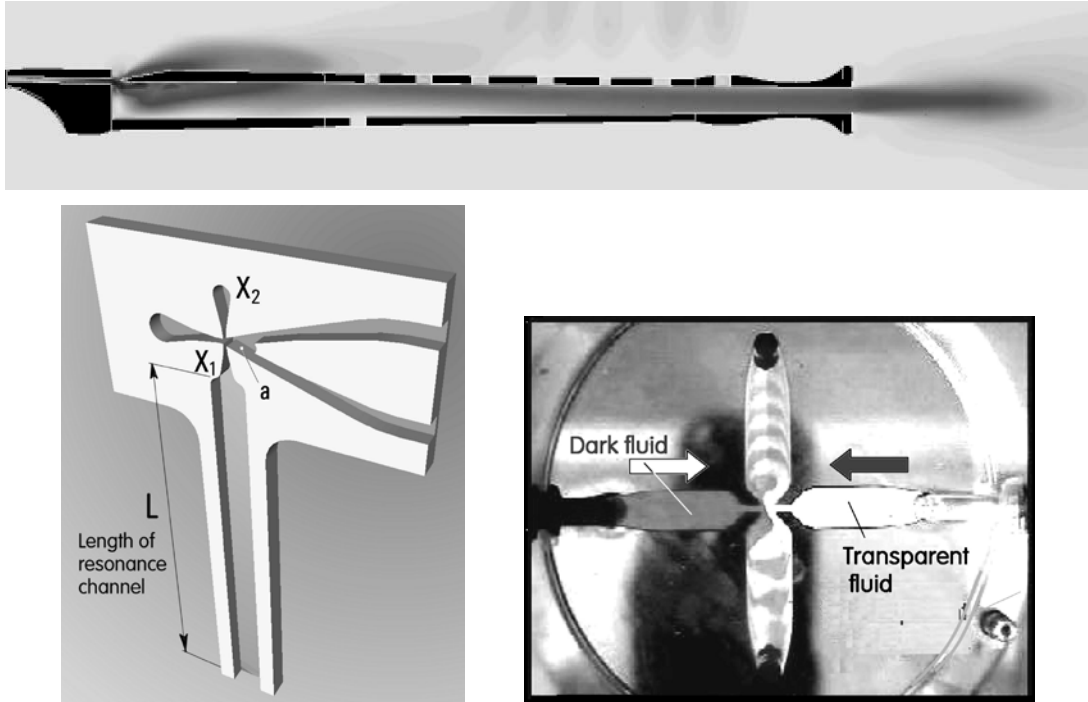
Fig. 10 (Top) Computed velocity field in a musical instrument - recorder flute [18]. Acoustic waves in the resonator are excited by the vortex shedding from a jet impinging upon an oppositely located sharp edge. The shedding, in turn, becomes periodic by the action of pressure waves reflected from the open end.

Fig. 11 (Bottom left) Author's oscillator developed for applications requiring high oscillation frequency at small flow velocities [19]. The basic component is a bistable Coanda-effect amplifier, with the switching action of feedback-loop flows is replaced by the action of pressure waves propagated and reflected in a quarter-wave resonator.

Fig. 12 (Bottom right) An example of oscillator based on the instability of colliding jets [20] (one of the fluids is coloured for visualisation of the process, the other one is transparent) Ref. [20] has actually identified in this device an internal feedback loop action.

This idea of fluidic oscillators was developed only recently [19]. It is intended for applications in control of flow by pulsatory jet-type actuators. This application requires rather high frequency of generated oscillation and yet not high jet velocities – these two requirements are mutually contradictory in what is obtainable with the classical feedback loop of Figs. 8 and 9. The new concept presented in Fig. 11, is based on the idea of the jet inside the amplifier switched by the action of acoustic waves travelling in a resonance channel. This channel is in Fig. 11 connected to one of the control nozzles, the nozzle labelled X_1. The other, bottom end of the resonance channel is open into the atmosphere. Also the other, opposite control terminal X_2 is open and allows for unrestricted inflow of air from the atmosphere. This opening of the control terminal X_2 is equivalent to giving preference to the opposite attachment wall a: the main jet always clings to it when the fluid flow starts. The low pressure at the attachment wall, which is the reason why the Coanda effect deflects the jet, is eliminated by the easy inflow of the atmospheric air nullifying the attachment. Even though the used amplifier is a standard symmetric one, this turns it into an effectively monostable device. The deflection of the jet issuing from the supply nozzle is caused by the impact of pressure waves. They travel through the resonance channel and return after a reflection from the open end. The delay in switching depends on the travel time of the pressure changes in the resonance channel. Thus the oscillation frequency is determined by the resonator length L (and on the acoustic propagation velocity). It does not depend on the air flow rate passing through the device. This sort of oscillators has among its ancestors whistles and similar musical instruments – as is shown by the example of recorder flute in Fig. 9. In a manner similar to the oscillator from Fig. 11 the frequency of the generated tone in the flute also depends on the length of the resonance tube, with the travelling waves reflected from the open tube end (or from the opening into atmosphere: the frequency may be changed by closing all but one of these exit openings by player's fingers).
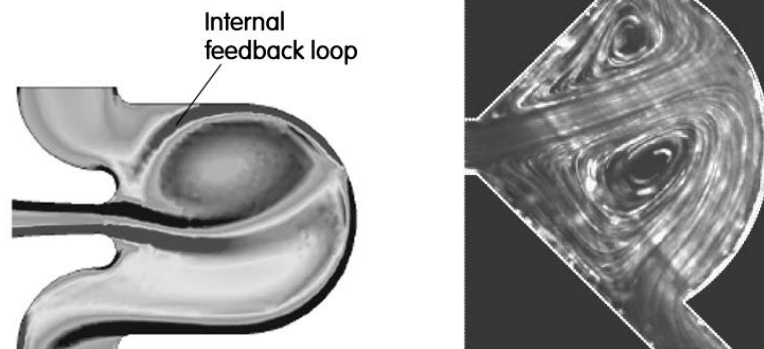
Fig. 13 (Left)   An inner feedback loop (a return flow tow2ards the nozzle) was identified in the flowfield also in this example (from [21]) of a jet oscillating upon impingement on a concave wall.

Fig. 14 (Right)   Another, perhaps even more convincing inner feedback loop, is seen in the visualised flowfield of an impingement on concave wall in [22].

There is a group of seemingly wholly dissimilar oscillator principles that is named under the common heading at the fifth line in the list of Fig. 1. Although perhaps not immediately apparent, the feature they share the feedback mechanism provided by vortices (which are often stationary, at least for the duration of a particular cycle).

A family of oscillator principles, not very commonly seen, utilises the fact that the stagnation point of collision of two mutually opposed fluid jets is unstable. Especially if the geometry is symmetric so that no jet is given a preference, the instability causes them to exchange their role in a periodic manner. One of applications is the small-scale no-moving-part oscillator developed by the present author [20] for mixing two reactants prior to their admission into a chemical microreactor. In one half of the oscillation period shown in Fig. 12 the dark-fluid jet from the left-hand nozzle is directed into one output, followed during the other half-period by the other, transparent reactant, This is a high-frequency device and since the periods are short, the flow in the output channels consists of interleaved layers of the two fluids. The oscillation depends on dynamic effects in the flowing fluids so that there is a lower limit of Reynolds numbers at which the device can operate. In experiments this limit was quite low, at Re ~ 30, which made this device well suited for the use in microfluidics [29]. Data from performed experiments with two different models in [20] are in agreement with very simple kinematic theory based on the idea of a feedback effect produced by vortices located on both sides of the jet.
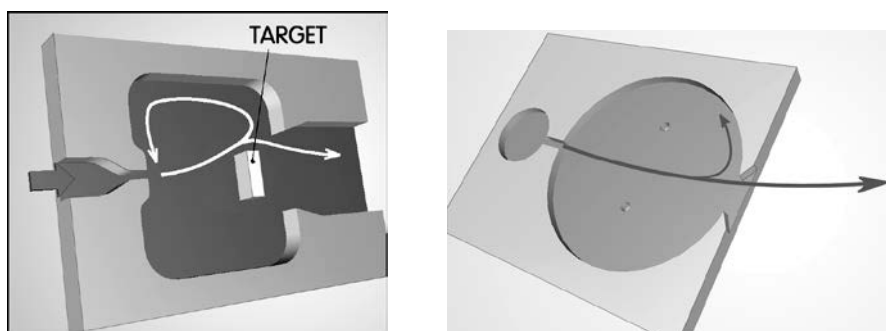

Fig. 15 Left)   The target-type oscillators are particularly popular in digital flowmeters based on counting oscillation cycles per unit of time (because of the Strouhal number constancy, the oscillation frequency is proportional to the flow rate).

Fig. 16 (Right)   The feedback flows may be "stripped" from the main jet by sharp edges positioned - on the mutually opposite sides - at the exit from the cavity. Again, the standing vortices (here stabilised by vent holes at their core) provide the feedback loop action.

Essentially the same mechanism of feedback by the recirculation provided by standing vortices is used in the oscillators characterised by jet impingement on an opposite convex wall. As shown in Figs. 13 and 14, the jet does not remain straight and performs self-excited lateral motions. The key role of the stationary vortices on both sides of the jet becomes discernible by flow visualisations. The next type mentioned in the list Fig. 1 are target-type oscillators, Fig. 15. In their usual flowmeter application they use an electric signal pick-up so that they do not need the two exits for bringing out the output flow pulsation - but this may be arranged easily. On one hand, these oscillators may be seen as related to the concave wall type. Since the basic effect is that of the vortices on both sides of the jet, the concave wall shape is not critical and the sideways flapping motion may exists even with the plane target face. There is, on the other hand, another possibility how to interpret the action, taking Fig. 5 as the starting point and considering the feedback flow as running here along the cavity walls rather than (as in Fig. 5) through a feedback loop channel. Similar obvious role of the standing vortices may be seen in the cavity of the case presented in Fig. 16.

2.2. The choice

Author evaluated the principles listed in the previous section an reached the following conclusions:

The requirement of good efficiency practically eliminates from consideration for the discussed application all principles the operation of which is based on impact and/or collision, in which the kinetic energy of the jet is practically dissipated – as is the case of the principles from Figs. 12, 13, 14, and 15 (or, in general, the case of vortical internal feedback loops).

The case of the negative slope, Fig. 2, was included into the survey for completeness but is also more or less out of question.. The only known realisation, with the vortex amplifier, cannot be used for the requested frequency range because the long spin-up time limits these amplifiers to rather slow processes. In general, it was considered not advisable to enter the field of exotic, little known oscillators like the negative-slope and Eccless-Jordan case: If they were really good, there would be certainly many more researchers attracted to them. Investing time and effort into an unusual oscillator might be contraproductive for the target of generating the microbubbles. Also, the mutual blockage principle of Fig. 3 is actually known applied only in the case shown in Fig. 4 – i.e. with the pair of vortex amplifier, the slowness of which was already mentioned as an argument against the case from Fig. 2.
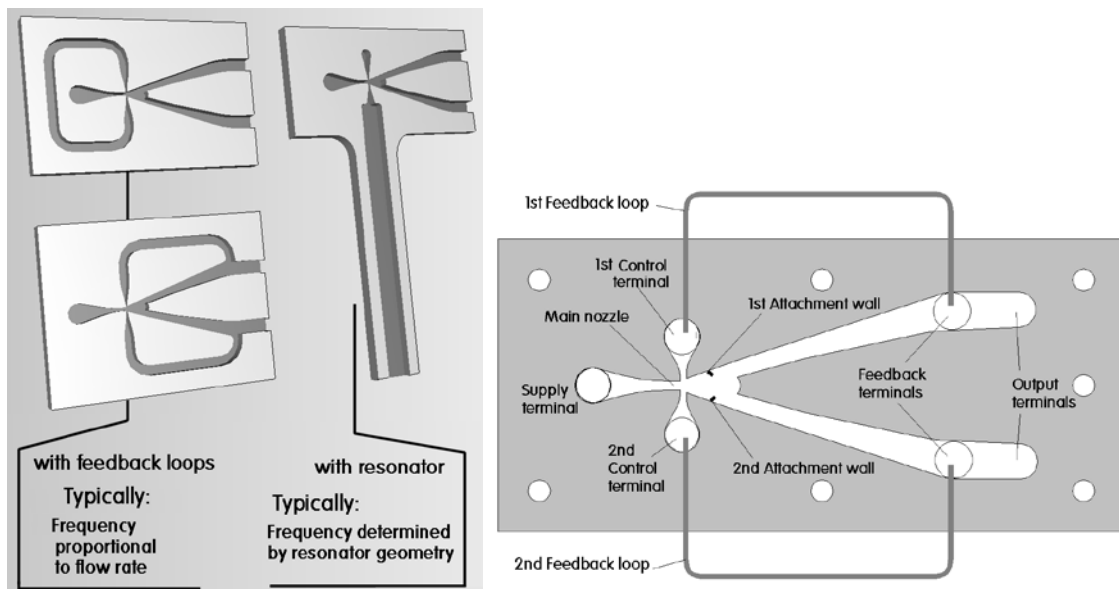

Fig. 17 (Left) After completion of the survey, the choice was practically limited to the three cases shown in this illustration. Note the different character regarding the variations of the frequency.

Fig. 18 (Right) An overall view of the plate in which the oscillator cavities were made in this author's device by laser cutting. The Warren oscillator type external feedback loops are outside of this plate plane – in connecting tubes that may be easily cut to various lengths for adjusting frequency. The two-loops version was found less sensitive to asymmetry of amplifier behaviour, which may arise due to manufacturing tolerances.

The elimination of the obviously unsuitable choices from the list in Fig. 1 actually left as acceptable possibilities the three layouts presented in Fig. 17. They all share the advantage of the easy adjustment of the oscillation frequency, which is determined by the length of the feedback component – which may be made (at least in the initial, laboratory test version) in the form of flexible tubes. Gradual cutting the tube to shorter and shorter length would increase the generated frequency in both the feedback loop as well as the resonance channel versions.

The basic component is in all three cases of Fig. 17 the unvented bistable jet-deflection amplifier with symmetric Coanda-attachment walls. It advantage is the attainability of low overall hydraulic losses: even though the air has to be accelerated in the main nozzle (this is necessary because the amplification effect is dependent on dynamic action in flowing air), there are no drastic changes of flow direction inside the interaction cavity (between the two attachment walls, Fig. 18, and immediately downstream there may be diffusers the small divergence angle of which should ensure reasonable pressure recovery. In fact the attachment to the wall results in decreasing the hydraulic loss, because the wall friction slows the jet much less than entrainment of outer stagnant fluid on the open jet boundaries. After all, it was on this version of fluidic amplifiers for which the present author performed am in-depth study [25] of pressure recovery.
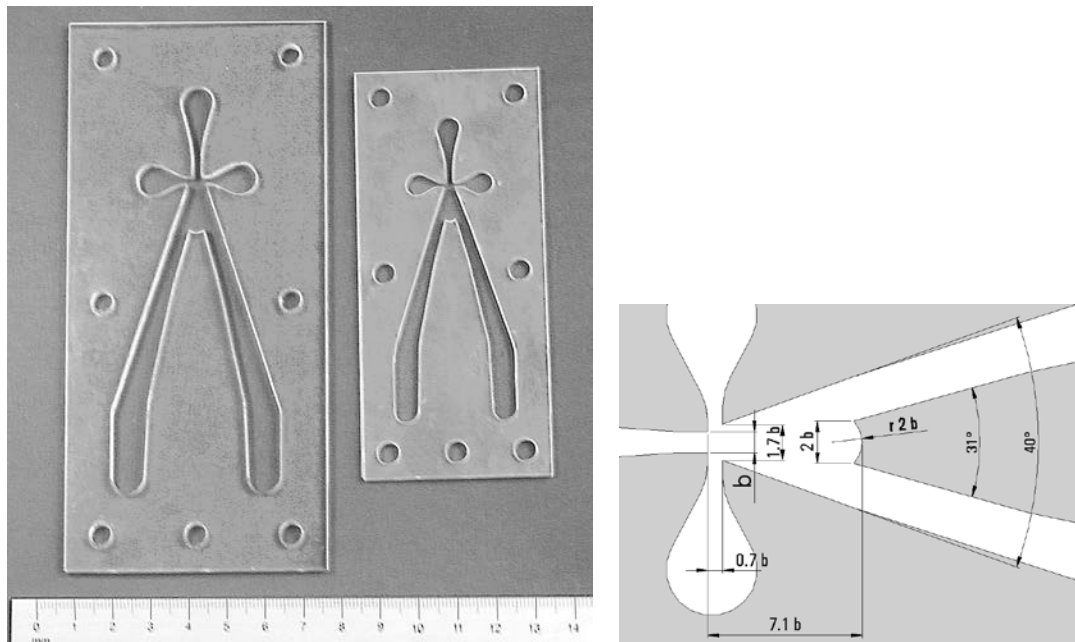

Fig. 19 (Left) Photograph of the base plates of the two oscillator models discussed in this paper. The larger version was made because the strange behaviour of the smaller version was considered to be a possible consequence of the imprecise laser cutting of the very small details.

Fig. 20 (Right) Ideal geometry of the core part of the oscillator. Two models were tested, with different sizes b of the main nozzle exit, to test whether the unexpected properties were due to too wide geometric tolerances of these fine details in the manufacturing by leaser-cutting.

Further examinations of the potential drawback and advantages finally resulted in selecting the feedback loop version according to Fig. 8 for conversion of the amplifier into the oscillator. The feedback loops are of the Warren's [17] two-loop configuration, Fig. 18 In the present initial, laboratory test version they are not in the form of channels cut in the pale (as in bottom left part of Fig. 17) but are made as silicone rubber tubes (of adjustable lengths, as mentioned above). In contrast to the constant oscillation frequency of the resonator feedback version (presented in the right-hand part of Fig. 17) it was expected that with the external-flow feedback the oscillator will exhibit the usual constant Strouhal number Sh property, i.e. the frequency directly proportional to the supplied air flow rate.

The nominal geometry of the most important part, the interaction cavity of the amplifier – where there are the smallest cross sections and hence the highest flow velocities – is presented in Fig. 20. because of the intended use with a small aerator model, the dimensions of the amplifier were chosen rather small. The workshop drawing magnitude of the width b of the main nozzle was 1.4 mm. The

oscillator did oscillate, but –as discussed in the next section – the behaviour did not correspond to any of the two expected cases in Fig. 17. In the search for possible causes, detailed measurements of the cavity dimensions have shown significant departures from the nominal values. In attempts at an improvement of the behaviour, the shapes as shown in Fig. 20 were slightly changed by light (and careful) filing with s fine file. No significant enhancement was found. In search for the reasons, too wide manufacturing tolerances of the laser cutting supplier were suspected and as a remedy was suggested ordering another cutting – a model that would be √2-times larger, i.e. $b = 2$ mm. The scaled-up main plate of the amplifier is shown at the left-hand side of the photograph Fig. 19. Also this oscillator did oscillate and could be used in the microbubble generation tests. Nevertheless the strange behaviour was again observed. Despite the laser cutting using simply the scaled-up AutoCAD drawing, the geometry of the small and the large model were not mutually completely similar. Due to manufacturing tolerances and the attempts at improvement by filing there were small dissimilarities of the shape. The real size of the main nozzle exit width were $b = 1.7$ mm for the smaller oscillator, and $b = 2.2$ mm for the larger one. Also the plate thicknesses were not simple scaled: their values were $h = 2$ mm (resultant in aspect ratio $h/b = 1.18$) for the small model and $h = 3$ mm (i.e. $h/b = 1.36$) for the larger one.

2.3. The strange oscillator properties

Until now, two versions - as presented in Fig. 17 - of the fluidic oscillator behaviour have been known and reported in literature. It is, on one hand, the constant Sh property, whereby the frequency of generated oscillation is proportional to the supplied flow rate. On the other hand, typical for switching controlled by the travelling pressure waves, is the behaviour characterised by the frequency not dependent on the flow rate. A very exceptional situation was observed in [10] as shown there in Fig. 18 of that paper: an oscillator with the single-loop (as on the top in the left side of Fig. 17) feedback exhibited the usual proportionality between the flow rate and frequency at small flow rates – but as the flow rate was increased, this behaviour was replaced by the other, constant-frequency resonance regime. This change in character was in [10] explained by the oscillation becoming locked to some resonant conditions.

What was found in the present case is wholly different. The frequency is not constant and increases linearly with increasing mass flow rate $\dot{M}$ [kg/s] — but this linear dependence is not homogeneous (so that Strouhal number is not constant) since there is a very large non-zero intercept value (i.e. the value obtained by extrapolation to zero flow rate). This character was found in both larger and smaller model, Fig. 19. In spite of the above mentioned slight geometric dissimilarities between them, the similar character of the behaviour called for comparison of the two models. To make such comparison possible, in Fig. 21, the dependence of frequency on flow rate was converted to dimensionless variables. On one hand it is Stokes number

$$Sk = \frac{f\,b^2}{\nu} \qquad \ldots (1)$$

and, on the other hand, Reynolds number

$$Re = \frac{w\,b}{\nu} = \frac{v\,\dot{M}}{h\,\nu} \qquad \ldots(1)$$

- where w [m/s] is the bulk velocity in the supply nozzle exit, ν [m^2/s] is air viscosity, v [m^3/kg] is its specific volume, and h is the depth of the cavities –

In terms of these variables, the experimental data points in Fig. 21 follow the straight lines

$$Sk = Slope\ Re + Sk_{intercept} \qquad \ldots (3)$$

The values of the two constants in eq.(3) $Slope$ and $Sk_{intercept}$, were found dependent on the relative length L of each of the two feedback loops. Graphically these dependences are presented in Fig 22 (the intercept value of the Stokes number) and Fig. 23 (where there are magnitudes of the slope from eq. (3). In spite of the scatter of the experimental data in these diagrams, the dependences are reasonably fitted by power-law straight lines in the used logarithmic scales. Quite surprisingly, the exponents in the power law expressions were found very near to integer values – so near that it is unlikely to be a mere chance. The diagrams also include the alternative power-law lines with the integer exponents (particularly the mutual agreement in Fig. 22 is so tight that the two straight lines are difficult to discern). In terms of these two expressions from Figs. 22 and 23, inserted into eq. (3), the data in Fig. 21 may be seen as obeying the universal law

$$Sk = B\,b/L\ Re + A\,\sqrt{b/L} \qquad \ldots (4)$$
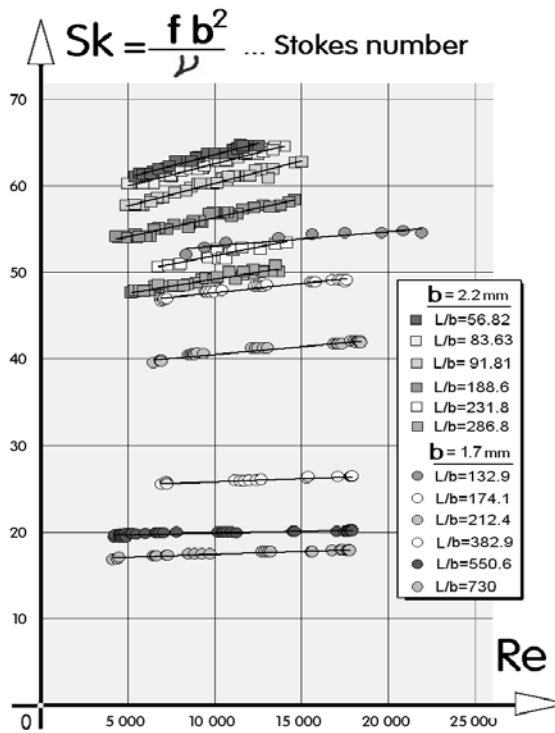
Fig. 21 Stokes number – proportional to frequency – was found neither constant nor linearly varying with Reynolds number. Both small and large model (Fig. 19) were found to behave in a mutually similar manner. Data points for a certain feedback loop length L are very well fitted by linear dependence determined by two parameters: slope and intercept.
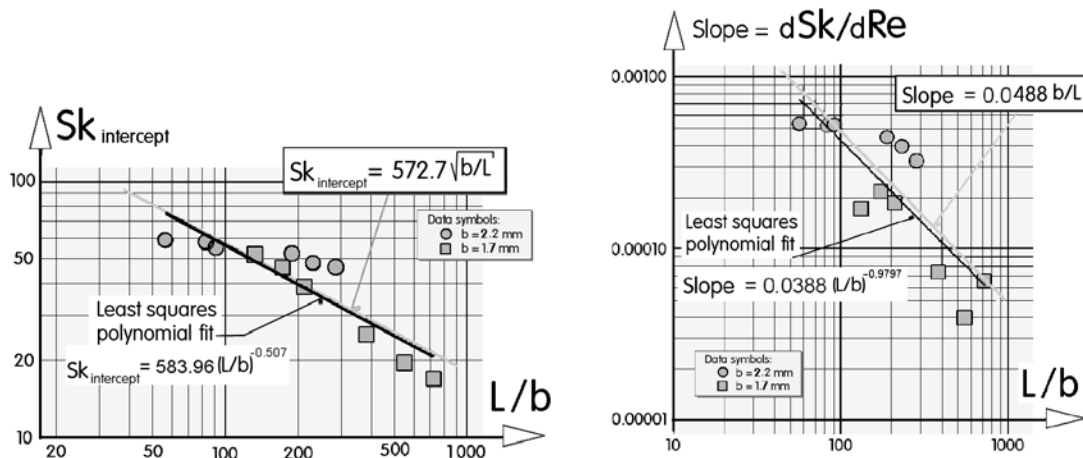

Fig. 22 (Left) The values of the intercept (i.e. extension of the straight line fitted to data upto the vertical axis in Fig. 21) were found to be inversely proportional to the square root of the relative loop length L/b.

Fig. 23 (Right) The other parameter of the linear fits through the data in Fig. 21, the slope of the line, may be reasonably fitted by inverse proportionality to the relative loop length L/b.

- where $A = 523$ and $B = 0.0488$.

Another alternative how to describe the discovered dependences is to write the expression for the generated frequency as

$$f = w\frac{B}{L} + \frac{A\nu}{b\sqrt{bL}}$$

... (5)

- again with the Strouhalian first term and the rather large second term characterising the non-zero intercept.

3   Conclusions

The key task in the investigated problem of generating gas microbubbles in liquids is the design of suitable fluidic oscillators. Author performed a detailed survey of available possibilities as listed in Fig. 1 and also used his previous experience from, e.g., [10, 19, 24, 25, and 28].   The finally chosen configuration is the bistable Coanda-effect amplifier with two Warren-type feedback loops. In model form it did perform the expected oscillation generation. When its behaviour was investigated, however, quite surprisingly, the behaviour of the oscillator was found to be rather strange – certainly agreeing with neither of the two alternative behaviour patterns known so far. There is a dependence of the oscillation frequency on the supplied gas flow rate – but this dependence is much weaker, a property that may be a useful in some other applications.

Acknowledgements

References

[1] Wu C., et al.: "Generation and characterisation of submicron size bubbles", Advances in Colloid and Interface Science, in Print, 2012

[2] Nash K. L., et al.: "Oxidative leaching of plutonium from simulated Hanford tank-waste sludges", Separation Science and Technology, Vol. 40, p. 1497, 2005

[3] Suslick K.S., Fang M., Hyeon T.: "Sonochemical synthesis of iron colloids", Journal of American Chemical Society, Vol. 118, p. 11960, 1996

[4] Prakash A., et al.: "Hydrodynamics and local heat transfer measurements in a bubble column with suspension of yeast", Biochemical Engineering Journal, Vol. 9, p.155, 2001

[5] Zimmerman W. B. J., Zandi M., Bandulasena H.C.H., Tesař V., Gilmour D.J., Ying K.: "Design of an airlift loop bioreactor and pilot scales studies with fluidic oscillator induced microbubbles for growth of a microalgae *Dunaliella salina*", Applied Energy, Vol. 88, p. 3357, 2011

[6] Zimmerman W.B.J., Tesař V., Bandulasena H.C.H.: „Towards energy efficient nanobubble generation with fluidic oscillation", Current Opinion in Colloid & Interface Science, Vol. 16, p. 350, 2011

[7] Zimmerman W.B. J, Tesař V.: "Bubble generation for aeration and other purposes", European Patent EP2081666, granted 19th Oct. 2011, published 26th Sept. 2012

[8] Jaliashvili T. A, Jaliashvili N. T., Darakhvelidze L.: „Method for induction synthesis of heat stress proteins (HSP) and production from herbaceous plants", Patent No. WO 00/70932, granted 30th Nov. 2010

[9] Attanasi E.D., Meyer R.F.: "Natural bitumen and extra-heavy oil", Survey of energy resources (22nd ed.), World Energy Council, p. 123, 2010

[10] Tesař V., Hung C.-H., Zimmerman W. B. J.: "No-moving-part hybrid-synthetic jet actuator", Sensors and Actuators, A: Physical, Vol. 125, p. 159, 2006

[11] Bouteille D.: "Fluid logic controls and industrial automation", ISBN-10: 0471091723, John Wiley & Sons, 1973

[12] Hanotu J., Bandulasena H.C.H., Zimmerman W.B.J.: " Microflotation performance for algal separation", Biotechnology and Bioengineering, Vol. 109, p. 1663, 2012

[13] Millman W.V., Mayer E. A.: „Vortex valve fluid oscillator", ES Patent Nr. 3674045, filed July 1970

[14] Eccles W.H., Jordan F.W., "Improvements in ionic relays", British Patent GB 148582, filed June 1918

[15] Zalmanzon L. A.: "Method of automatically controlling pneumatic or hydraulic elements of instruments and other devices", US Patent 3,295,543, filed Feb 1960

[16] Warren R.W.: "Fluid oscillator", US Patent 3,016,066, filed 22nd Jan 1960

[17] Warren R. W.: "Negative feedback oscillator", US Patent 3,158,166, filed 7th Aug. 1962

[18] Fuss S., Marburg S.: „Numerical computations of a recorder flute", Proc. of 20th International Congress of Acoustics, Sydney, 2010

[19] Tesař V., Zhong S., Fayaz R.: „New fluidic oscillator concept for flow separation control", AIAA Journal, in Print , DOI: 10.2514/1.J051791

[20] Tesař V.: "Oscillator micromixer", Chemical Engineering Journal, Vol. 155, p. 789, 2009

[21] Uzol O., Camci C.: "Experimental and computational visualization and frequency measurements of the jet oscillation inside a fluidic oscillator", Proceedings of 4th International Symposium on Particle Image Velocimetry, paper 1029, Göttingen, 2001

[22] Sun C.-L., Sun C.-Y.: "Effective mixing in a microfluidic oscillator using an impinging jet on a concave surface", Microsystem Technologies, Vol. 17, p. 911, 201181)

[23] Tesař V., Trávníček Z., Kordík J., Randa Z.: „Experimental Investigation of a Fluidic Actuator Generating Hybrid-Synthetic Jets", Sensors and Actuators A, Vol. 138, p. 213, 2007

[24] Tesař V., Bandalusena H.: „Bistable diverter valve in microfluidics", Experiments in Fluids, Vol. 50, p. 1225, 2011

[25] Tesař V.: „Mechanism of Pressure Recovery in Jet-Type Actuators", Sensors and Actuators A-Physical, Vol. 152, p.182, 2009

[26] Tesař V,: "Fluidic oscillator devices based on the ' Aerodynamic paradoxon' ", Proc.of Conf. " Flow Induced Vibration", Praha 2008

[27] Tesař V.: "Investigations into the Possibilities of Applying the 'Aerodynamic Paradoxon' Principle in Fluidic Devices" , In *Proc. of the IVth Intern. Fluidics Conf.*, Varna, Bulgaria, 1972

[28] Tesař V.: "Výměník tepla s fluidickým ústrojím k intenzifikaci přestupu" (Heat exchanger with fluidic facility for heat transfer intensification – in Czech), Czechoslovak Patent Nr. 262367, filed Dec. 1986

[29] Tesař V.: "Pressure-driven microfluidics", monograph, ISBN-10: 1596931345, published by Artech House Publishers, Norwood, MA 02062 USA

[30] Agarwal A., Ng W.J., Liu Y.: "Principle and applications of microbubble and nanobubble technology for water treatment", Chemosphere, Vol. 84, p. 1175, 2011

[31] Takahashi M., Ishikawa H., Asano T., Horibe H.: "Effect of microbubbles on ozonized water for photoresist removal", Journal of Physical Chemistry C, Vol. 116, p. 12578, 2012

[32] Xu Y., Liu H., Yan D., Ji Z.:"Bubble size measurement of deinked pulp flotation column", Paper Science and Technology, Vol. 25, p. 115, 2006